IOP Publishing European Journal of Physics
Eur. J. Phys. **41** (2020) 025304 (14pp) https://doi.org/10.1088/1361-6404/ab5bf9

Measuring the Raman spectrum of water with a smartphone, laser diodes and diffraction grating

P Onorato and L M Gratton

Department of Physics, University of Trento, Via Sommarive 14, I-38123 Povo (TN) Italy

E-mail: pasquale.onorato@unitn.it

Received 25 September 2019, revised 13 November 2019
Accepted for publication 26 November 2019
Published 10 February 2020

Abstract

We show how low-cost apparatus based on the use of commercial laser diodes, inexpensive diffraction transmission gratings coupled with a smartphone camera, can be assembled and employed to quantitavely measure the wavelengths of photons scattered inelastically as a consequence of the Raman effect. In particular, we measured the Raman shift of water stimulated by violet and green laser radiation.

Keywords: Raman effect, spectroscopy, low-cost experiment, physics education

(Some figures may appear in colour only in the online journal)

Introduction

The absorption and emission of electromagnetic radiation are fundamental concepts in science with a wide range of technological applications and pedagogical implications. From an experimental point of view, measurements of optical spectra to study the emission and absorption of light by atoms and molecules have played an important role in atomic physics since the end of nineteenth century.

In the last few years, spectroscopy has also started to play a central role in physics education research (PER), which identified that atomic spectra constitute a golden opportunity to study the concepts of quantum mechanics that teachers and students tend to form [1]. In fact the interpretation of atomic spectra requires a correct conceptualization of the quantization of energy both in the microscopic constituents of matter and in electromagnetic radiation, in addition to a model for explaining the interaction between them.

Thus measurements of optical spectra are particularly engaging for undergraduate students and prospective physics teachers also with the aim of understanding the stellar structure and evolution [2, 3]. More in general, some research in physics education [4] showed how applied optics offers a playground to teach fundamental concepts of radiation–matter interaction through interdisciplinary experimental activities.

In recent years, several inexpensive educational setups, based on the employment of consumer digital photocameras (webcams, compact cameras or smartphones), were proposed for spectral measurements [5–11], e.g. for analyzing fluorescent materials [12–15]. Most of these devices are based on cheap diffraction gratings.

Moreover, in the last decade low-cost laser pointers, handheld devices with a laser diode emitting a very narrow coherent low-powered laser beam of visible light, are easily available. These devices emit light at some given wavelengths corresponding to different colors (red, orange, yellow, green, blue and violet).

We combine the use of digital cameras as detectors and laser pointers as sources to investigate the light emitted by a material; here, water, when it is irradiated with a monochromatic laser to produce a spectrum consisting of scattered electromagnetic radiation at many different wavelengths.

In this line, we designed an experimental setup for educational purposes, which can be assembled very quickly from simple materials and allows performing wavelength measurements with good accuracy (measurements have uncertainty below 4 nm as obtained from the appendix). In this paper, we focus on how this apparatus can be used for quantitative measurements of the wavelength of the scattered light from a target of water.

The relevant phenomenon, which can be discerned by these experiments focused on the inelastic scattering is the Raman scattering [16]: when photons are scattered by a material, the largest part of them are elastically scattered (Rayleigh scattering), and the scattered photons have the same energy (wavelength) as the incident photons but different directions. However in some materials, a small fraction of the photons are scattered inelastically, with the scattered photons having an energy different from, and typically lower than, those of the incident photons. These photons, located around the laser beam in transverse directions, can be Raman-scattered photons or fluorescent-emitted photons. In the Raman scattering the incident photon energy excites vibrational modes of the molecules, yielding scattered photons that are diminished in energy by the amount of the vibrational transition energies. A spectral analysis of the scattered light under these circumstances will reveal spectral satellite lines below the Rayleigh scattering peak at the incident frequency. Such lines are called '*Stokes lines*' [17][1].

A simple energy level diagram that illustrates the electronic states of two molecules and the transitions between these states comparing the Raman effect and the fluorescence is shown in figure 1. Both fluorescence and Raman scattering involve the irradiation of a sample with light and the detection of the light emitted by the sample. The main difference between these phenomena is that the wavelength of fluorescence emission is generally independent of the wavelength of the exciting light (see figure 1). In contrast, the wavelength of Raman light scattering increases with increasing wavelength of the exciting light and the Raman-scattered light exhibits a frequency shift usually expressed with respect to wavenumber (in unit cm^{-1}) proportional to the energy shift.

[1] In this work we will neglect the *anti-Stokes lines*. These lines appear above the incident frequency when there is significant excitation of vibrational excited states of the scattering molecules. In this case the vibrational energy is added to the incident photon energy but these lines are generally so weak that our experimental setup is unable to reveal them. We will also neglect the effects of the light polarization, which sometimes could be very relevant. In fact when a material is exposed to linearly polarized light, it may interact differently than it does for depolarized light depending on how the material is oriented relative to the polarized light axis.

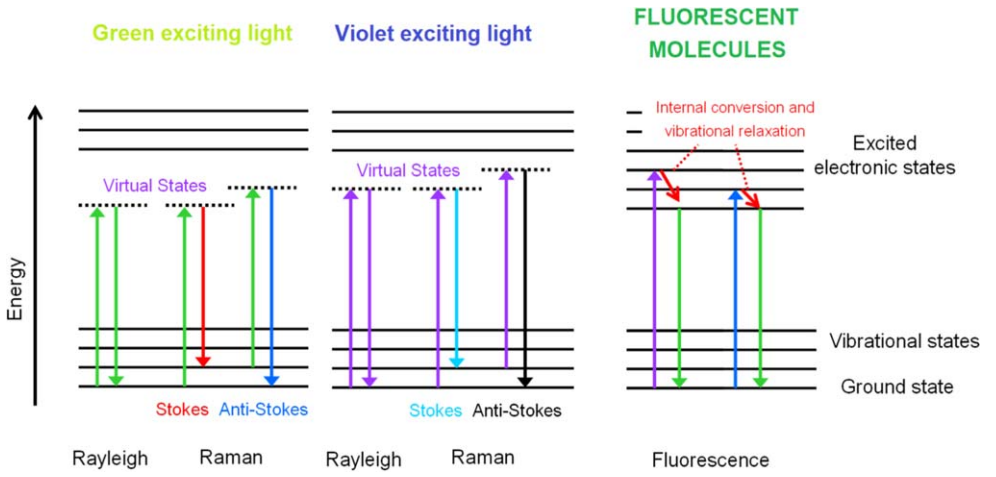

Figure 1. A simple energy level diagram (Jablonski diagram) useful to discuss Raman effect and fluorescence.

In more detail, when light (left green arrows and violet arrows in figure 1) is incident on a molecule at an initial ground state, it can be prompted to a virtual energy level (very short-lived, unobservable quantum state) and quickly return to the initial state. Since there is no energy level transition, photons are emitted at the same energy as the incident light (Rayleigh scattering). Raman scattering also involves an intermediate virtual energy state even if, in this case, there is an energy transfer between the incident light and molecule. The Raman emission occurs as two possible outcomes, Stokes or anti-Stokes scattering. Stokes scattering occurs when a molecule is initially in the ground state, is transitioned to a virtual energy level and then relaxes to an excited state (thus for a green absorbed photon we have a red emitted one and for a violet absorbed photon we have a blue emitted one). Anti-Stokes scattering occurs when a molecule is initially in an excited state prior to irradiation with and is promoted to a virtual energy level, then relaxes to the ground state with after scattering (thus for a green absorbed photon we have a blue emitted one and for a violet absorbed photon we have a UV emitted one). Also fluorecence photons irradiated on the substance cause the transition of electrons when they have a sufficient amount of energy (right blue and violet photons in figure 1) in molecular orbitals from the quantum ground state to an excited state with higher energy by the absorption process. Subsequently, the energy can be emitted through photons, with a lesser energy than the absorbed ones (green photons from the final excited to the ground state), and converted in thermal energy by lattice quantum vibrations (phonons) with the mechanism labelled as internal conversion and vibrational relaxation, a mechanism which involves excited states [18].

In this paper, we illustrate a low-cost apparatus that employs commercial laser diodes as light sources, and, as detectors, inexpensive diffraction transmission gratings coupled with the smartphone camera. This setup can be easily assembled and employed to quantitatively measure the wavelengths of photons scattered inelastically as a consequence of the Raman effect and both the equipment and the proposed experiments seem suitable for introductory physics students and high school students laboratory work.

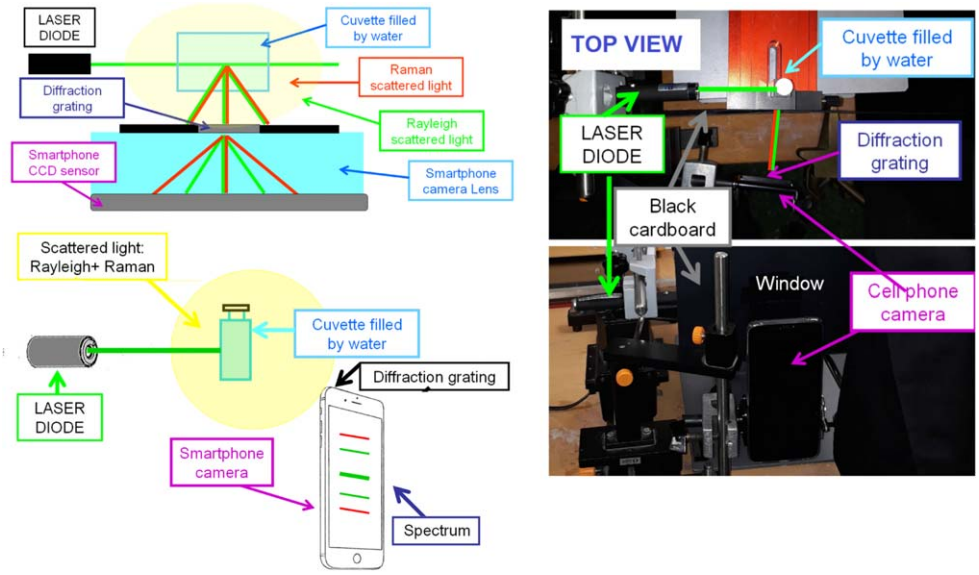

Figure 2. The spectrographs setup. We show the top and side views. The laser beam enters the water in the cuvette and the scattered light is detected by the smartphone camera after passing the diffraction grating.

Equipment

In figure 2 we show the apparatus. The equipment employs a 300 l mm^{-1} transmission grating and a cellphone *camera,* the smartphone required to perform the experiment has to be able to acquire, in manual mode, long-exposure photos, i.e. images taken with a camera whose shutter remains open for a long time. The amount of light that reaches the image sensor is proportional to the exposure time, thus with long exposure the sensor is able to capture more light, which leads to bright images. Moreover it is advantageous that a cellphone is also able to save the photos as raw files[2]. Thus we use a Huawei MATE20PRO, but some models of cell phones and many digital cameras have these requirements.

A transmission grating is attached with adhesive tape to the cellphone's photo camera. The cellphone is fixed using a selfie stick and the camera frames a cuvette filled by distilled water. A laser beam enters the cuvette from the left so that the camera gathers the light scattered orthogonally to the direction of the laser. A black cardboard screen with a narrow window (3 mm width) is placed between the cuvette and the cellphone just to reduce the scattered light mainly coming from the cuvette's edges. The transmission gratings disperse the beam of light into spectral lines with different colors at different angles, thus the spectrum is acquired as a digital photo both in raw and jpeg formats.

The use of laser light ensures that only approximately collimated light is focused by the camera lens on the detector so that it does not need the narrow slit usually required for homemade spectrometers [7, 8].

[2] Raw file analysis allows the adding, subtracting and averaging of many images taken in the same condition in order to increase the signal-to-noise ratio. The latter procedure is not possible with files saved in jpg format, as the camera processes the native images in a different way to compress them to jpg files.

Both the laser diodes are easily available and are very cheap, with wavelengths of 405 nm and 532 nm.[3] The violet laser produces a laser beam with an output power smaller than the green one; in fact the Raman scattering cross-section of liquid water for the excitation wavelength corresponding to green is many times smaller than for the excitation wavelength of violet light as reported in [20] where the authors presented measurements of the wavelength dependence of the 3400 cm^{-1} Raman scattering cross-section of liquid water for excitation wavelengths between 215 and 550 nm. The latter study showed how the cross-section reduces when the excitation wavelength increases. Thus the Raman scattering cross-section of liquid water for the excitation wavelength corresponding to green is many times smaller than for the excitation wavelength of violet light. Thus the exposure time will be larger for the green laser.

Calibration

For the wavelength calibration of the spectrograph, we use two subsequent orders of diffraction (the first and the second) and we base the measurements on the nominal wavelength of the laser diodes. The small angle approximation, which allows us to assume a linear dispersion ($\frac{\Delta\lambda}{\Delta pxl} = const.$ where λ is the wavelength in nm and *pxl* is used for pixels) a priori is not exactly established, even more so if we use two subsequent orders of diffraction for calibration. Thus, as we show in the appendix, using a spectrograph similar to the one proposed in [7, 8] and a fluorescent lamp with several lines, we can prove that the 300 l mm^{-1} grating ensure a good linear dispersion up to the third order of diffraction and we measure the dispersive power $\frac{\Delta\lambda}{\Delta pxl} \approx 1\frac{\text{nm}}{pxl}$.

When we will analyze the raw photos (thanks to a ImageJ software [21]) we can straightforwardly obtain a measure of the light intensity (*gray value*) for each pixel [22], the same results can be roughly obtained starting from the RGB value in color space. To obtain the measurement of light *luminance* from RGB values for a typical gamma-corrected (jpeg) image generated by a photo camera, we use the formula implemented in tracker video analysis [15]:

$$Y_{\text{measured}} = 0.2126\, R^{\gamma} + 0.7152\, G^{\gamma} + 0.0722\, B^{\gamma}, \tag{1}$$

where Y is a measure of luminance, which is proportional to emitted light intensity per unit area, and $\gamma = 2.2$ is the γ-correction factor (see also [7, 8]) expressing how the luminance on the screen depends on the 8-bit RGB color values [23][4].

However the value of light intensity obtained, both from the Jpeg and from raw image, also depends on the overall response of the apparatus (CCD camera, lenses and so on), therefore we should evaluate the relative sensitivity [24] (spectral response) of the apparatus by measuring the light spectrum from a known source. This deep analysis of the images is beyond the aims of this work where we just focus on the wavelengths measurements.

[3] These Class 3B lasers, where output power is between 5 and 499 milliwatts, are hazardous for eye exposure. They can heat skin and materials but are not considered a burn hazard. Thus, the use of laser protective eyewear is recommended especially when the experiments are done by students. Even if the sellers (typically found on the websites of giants of the ecommerce industry) declare that these laser pointers have power less than 5 mW we employed the 1918-*C*—Newport Optical Power Meter to measure the actual power. We found ≈25 mW for the laser pointer at 405 nm and ≈180 mW for the 532 nm one. For the latter laser pointer we also introduced a Schott type IR filter (the S-KG whose technical characteristics are reported in [19] with the aim of measuring the visible fraction of the emitted radiation and we obtain just 28 mW. Since the low-cost commercial laser diodes could emit unexpected and hazardous non-visible radiation the laser diodes have to be carefully analyzed before using them with students. When it is needed filters can be used to cut off the unwanted radiation (here a Schott-type filter for IR radiation) students always need to be provided with the appropriate protection goggles.

[4] This is only true if the signal is above a threshold value while measurements based on jpeg images are ineffective and overtaken by noise when the signal is weak, as often happens for the Raman emission.

Measurement and results

In order to detect the Raman emission, we use the setup in figure 2 and we employ both green and violet lasers as light sources.

Figure 3(A) shows the jpeg spectra with an exciting laser at 405 nm, acquired with a long exposure (10 s and 1000 ISO). Figure 3(B) shows the jpeg conversion of a raw image[5] obtained in the same experiment (10 s and 1000 ISO), processed by employing ImageJ, by summing four raw photos and subtracting the background (the background measurements were done just by closing the narrow window in the black cardboard screen). The latter raw file can be analyzed straightforwardly by using ImageJ to obtain the gray value versus position (figure 3(C)).

In both images there are some violet spectral lines corresponding to the different diffraction orders of the laser source (see figure 3(A), where we underline the different orders of the laser light). Once we acquire the pictures of the spectral lines, we can accurately measure the positions of their peaks by using the free video analysis software Tracker [15]. Comparing the experimental findings with the known wavelength of the laser times the order of diffraction we can obtain the calibration curve which represent the peak positions (measured in pixel) *versus* the known wavelength. These curves are adequately fitted by straight lines as shown in the appendix ($R^2 > 0.998$ for the linear regression of position versus order of diffraction).

Thus from each jpeg image analyzed with Tracker and from each raw file series (four images of the spectrum and four images of the background) we can obtain from 1 to 4 (left-right and first-second order) different values of the wavelength corresponding to the Raman peak. Typical data acquired in many trials are reported in table 1.[6] The wavelengths were obtained starting from the plots like the ones in figure 3(C) by measuring the positions of the peaks (maximum values) and calibrating using the known laser's wavelength. Since unavoidable random errors affect the measurement mainly caused by inherently unpredictable fluctuations in the experimental apparatus, we obtain a significant spread of data set coming from repeated measurements.

Sometimes in the photos we notice a small deviation from the horizontal ($\approx 1.5^\circ$ in figure 3). This effect is due to a small misalignment between the grating and the laser beam. However the analysis with software such as Tracker allows us to correct the errors in estimating the peaks' wavelengths.

In figure 3(C) we also can observe that the spectrum is not symmetric about the central peak. This is mainly due to the fact that we employ blazed gratings [25] (also called echelette gratings or sawtooth gratings), a special type of transmission diffraction grating that is optimized to achieve maximum grating efficiency in one given diffraction order. Since the grating lines possess a triangular, sawtooth-shaped cross-section, forming a step structure, there is a left-right asymmetry mainly clear in the intensity of transmitted light.

From the data reported in the left sector of table 1 we can evaluate the Raman wavelength for the violet (405 nm) stimulating source as $\lambda = 469 \pm 5$ nm.

Raman shifts are typically reported in wavenumbers, which have units of inverse length. To convert between spectral wavelength and wavenumbers of shift in the Raman spectrum, we use the relation

[5] This is not the file analyzed to obtain the measurements in figure 2(C) and in table 1. The latter data was acquired straightforwardly analyzing the raw files with ImageJ.

[6] Once calibrated, the spectrograph the Raman lines position can be measured. In table 1 we report the results obtained by analyzing five different trials and measuring up to four peaks (first- and second-order, left and right) both using raw and jpeg images.

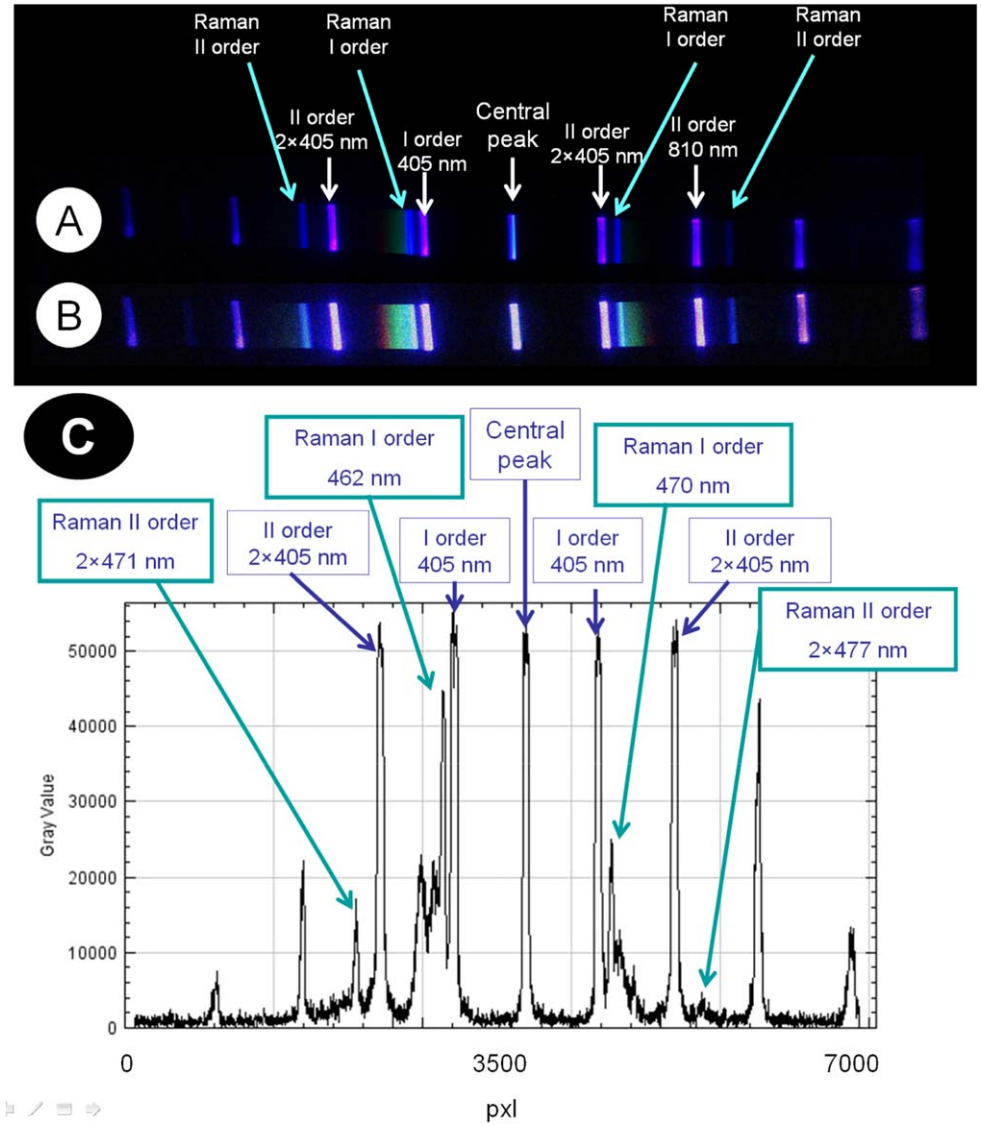

Figure 3. Spectra acquired with the smartphone camera for the exciting laser at 405 nm. (A) The jpeg spectra acquired with a long exposure. The Rayleigh 'violet' line is diffracted and visible up to the IV order. The Raman line 'blue' is just visible up to the II order. (B) The jpeg conversion of a raw image obtained in the same experiment, processed by employing ImageJ, by summing four raw photos and subtracting the background. The same lines of panel (A) are visible. (C) The ImageJ analysis of the raw file: the gray value versus position shows clearly four orders of the Rayleigh diffraction and two orders of the Raman peak. This kind of analysis, after a wavelength calibration, enable us to find four measurements of the Raman peak wavelength.

$$\Delta\nu = \left(\frac{1}{\lambda_0} - \frac{1}{\lambda_1}\right) \tag{2}$$

where $\Delta\nu$ is the Raman shift expressed in wavenumber, λ_0 is the excitation wavelength, and λ_1 is the Raman spectrum wavelength. Most commonly, the unit chosen for expressing

Table 1. Data of the wavelengths of the Raman peak. Results of measurements obtained using different photos.

Raman peaks (nm)		Trial		Raman peaks (nm)		Trial	
Source 405 nm	471	I order right	Measure 1 Raw file	Source 532 nm	641	I order right	Measure 1 Raw files
	462	I order left			636	I order left	
	470	II order right			639	II order right	
	477	II order left			640	II order left	
	465	I order right	Measure 2 Raw file		637	I order right	Measure 2 Raw file
	467	I order left			640	I order left	
	474	II order right			641	I order right	Measure 3 Jpeg file
	475	II order left			637	I order left	
	465	I order right	Measure 3 Jpeg file		645	I order right	Measure 4 Jpeg file
	460	I order left			650	I order left	
	465	I order right	Measure 4 Jpeg file		641	I order right	Measure 4 Jpeg file
	468	I order left			636	I order left	
	478	I order right	Measure 4 Jpeg file				
Peak wavelength $\lambda = 469 \pm 5$ nm				Peak wavelength $\lambda = 641 \pm 4$ nm			
Raman Shift $3.4 \pm 0.2 \times 10^3\,\mathrm{cm}^{-1}$				Raman Shift $3.2 \pm 0.1 \times 10^3\,\mathrm{cm}^{-1}$			

wavenumber in Raman spectra is inverse centimeters (cm^{-1}). The value of $\lambda = 469 \pm 5$ nm corresponds to a Raman wavenumber $\Delta\nu_{Blue} = 3.4 \pm 0.2 \times 10^{-3}\,cm^{-1}$.

The uncertainty in the measurement of the position of the Raman peak is smaller than the experimental width observed in the spectrum (see figure 3(C)). In fact the full width at half maximum (FWHM) is typically larger (10–20 nm) than the uncertainty obtained by the statistical analysis (5 nm).

Figure 4(A) shows the jpeg spectra with exciting laser at 532 nm, acquired with a long exposure (30 s and 1000 ISO). The image was analyzed straightforwardly by using Tracker to obtain the luminance versus position (figure 4(C)). Figure 4(B) shows the jpeg conversion of a raw image obtained in the same experiment, processed by employing ImageJ, by summing four raw photos and subtracting the background. In this image we can also distinguish the II order Raman, which is not detectable in the jpeg photos.

In the photo there are green spectral lines corresponding to the different diffraction orders of the laser source (also here we underline the different orders of the laser light). Then we can notice that the spectral line, due to the Raman scattering, is now in the red region of the spectrum. The comparison of the different colours of the Raman lines (blue and red) when we change the laser source shows how the Raman scattering is different from the typical photoluminescence phenomena. In fact in the Raman scattering the wavelength of the scattered photon is proportional to the wavelength of the excitation photon.

Also in this case we acquired many photos both in jpeg and raw format. Thus from each jpeg image analyzed with Tracker [15] and from each raw file series analyzed with ImageJ [21] we can obtain different values of the wavelength corresponding to the Raman peak. Thus also in this case we obtain a tenth of measurements and typical data acquired in many trials are reported in table 1. Notice that in this case we were never able to distinguish the II order Raman lines.

From the data reported in the right sector of table 1 we can evaluate the Raman wavelength for the green (532 nm) stimulating source as $\lambda = 641 \pm 4$ nm. This value corresponds to a Raman wavenumber $3.2 \pm 0.1 \times 10^{-3}\,cm^{-1}$ compatible with the one obtained for the violet laser.

Also in this case the uncertainty in the measurement of the position of the Raman peak is smaller than the experimental width observed in the spectrum (see figure 4(B)). In fact the full width at half maximum (FWHM) is typically larger (10 nm) than the uncertainty obtained by the statistical analysis (4 nm).

Finally we summarize all the results obtained above in order to compare the Raman shift measured with our rudimental apparatus and the one known from literature [26, 27]. Thus with the aim of depicting our results we plot a Gaussian function depending on the Raman shift (we use the Gaussian function following the authors of [27] who employed this kind of function for the fit of the asymmetric *O-H* stretch band around $3400\,cm^{-1}$ in liquid water), centred in the mean value of the Raman shift and with a width corresponding to the average width of the peaks shown in figures 3 and 4. In such way all our results can be outlined in a plot in the plane Raman shift intensity. Therefore in figure 5 we plot the function $g(\Delta\nu) = G_0 e^{-\frac{(\Delta\nu-\Delta\nu_0)^2}{2\sigma^2}}$, which approximates the Raman peak as a function of the Raman shift. This function is centred in the mean value of the two measurements as they result from equation (2). Thus the center is placed at $3.3 \times 10^3\,cm^{-1}$. The FWHM can be evaluated as $0.4 \times 10^3\,cm^{-1}$, thus starting from the properties of the Gaussian function, FWHM $= 2\sqrt{2\ln 2}\,\sigma \approx 2.355\sigma$, we estimate $\sigma \approx 0.2 \times 10^3\,cm^{-1}$.

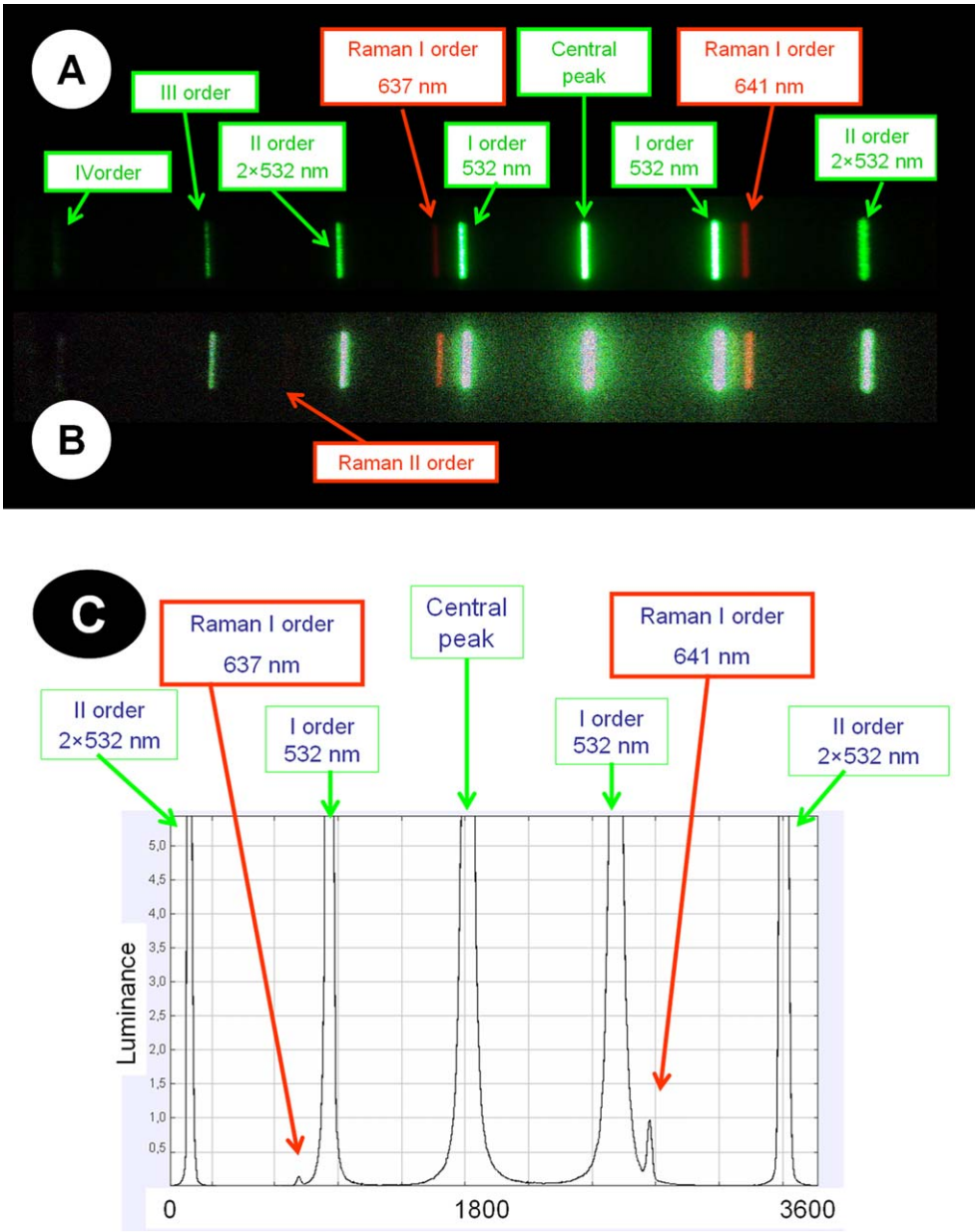

Figure 4. Spectrum acquired with the smartphone camera for the exciting laser at 532 nm with a long exposure (30 s and 1000 ISO. The Rayleigh 'green' line is diffracted and visible up to the IV order. The Raman line 'red' is just visible at I order in the jpeg file (A) while can be observed in the processed raw image (B). (C) The Tracker analysis of the jpeg file: the luminance Y versus position shows clearly four orders of the Rayleigh diffraction and 1 order of the Raman peak. This kind of analysis, after a wavelength calibration, enable us to find two measurements of the Raman peak wavelength.

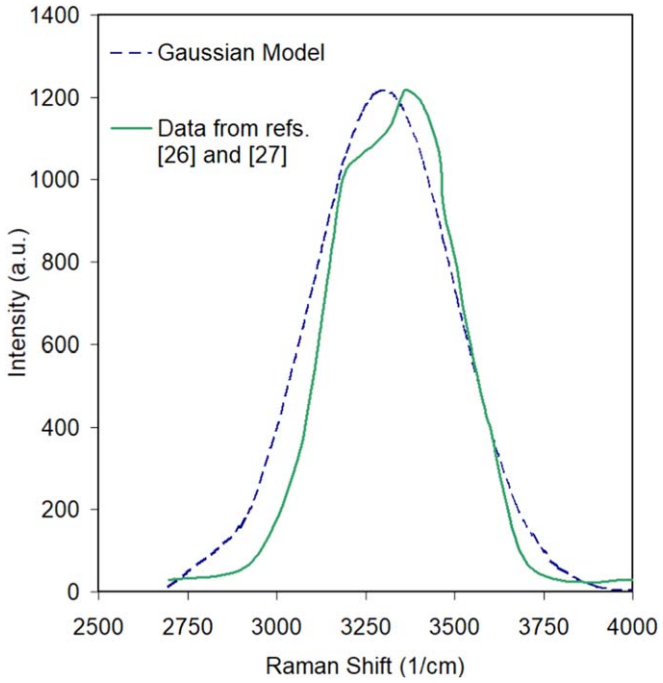

Figure 5. Green line. Raman scattering spectrum of pure water from the literature [26, 27]. The shoulder at $\sim$3250 cm^{-1} corresponds to the asymmetric –OH stretch, and the most intense feature at $\sim$3410 cm^{-1} corresponds to the symmetric –OH stretch [28]. The results of our measurements are summarized in the Gaussian plot, which approximate the light intensity versus the Raman shift just using the average position of the peak and the average linewidth. The Gaussian peak centered at 3.3 $\times$ 10^3 cm^{-1} has a FWHM $\approx$0.4 $\times$ 10^3 cm^{-1}Z.

In figure 5 the Gaussian function that summarizes our measurements is finally compared with the Raman spectrum of the water as it is reported in literature [27]. The asymmetric O-H stretch band around 3400 cm^{-1} is often broken down into a few Gaussian peaks, i.e. the Raman spectra can be deconvoluted into some peaks with two main subbands at $\sim$3250 cm^{-1} (asymmetric –OH stretch), and $\sim$3410 cm^{-1} (symmetric –OH stretch [28]). These peaks cannot be resolved or distinguished using our rudimental apparatus where the spectral lines are large and the uncertainties are huge. In figure 5 we just show that a one-peak Gaussian function built with our experimental parameters (dashed line in figure 5) matches well the experimental data of [27].

Conclusions

In summary, we have discussed how a low-cost apparatus based on the use of commercial laser diodes and inexpensive diffraction transmission gratings coupled with a smartphone camera, can be assembled. This homemade apparatus provides a simple way to perform quantitative measurement of the frequency properties of light, which in current classrooms is either done with expensive equipment, or only talked about but never experienced.

We employed this simple setup to quantitatively measure the wavelengths of light scattered inelastically as a consequence of Raman effect. Thus, after a calibration, we measured the Raman shift of water stimulated by violet and green laser radiation obtaining values of the Raman shift with small uncertainty (few nanometers) in good agreement with the results known from the literature. Thus the experiment proposed seems suitable for introductory physics students' and high school students' laboratory work, and the advantages of our device in terms of the potential wide spreading in high school and undergraduate laboratory courses are manifest.

Appendix. A wavelength calibration and linear dispersion

In figure A1 we show the apparatus that employs a $300\,\mathrm{l\,mm^{-1}}$ transmission grating used to verify the linear dispersion of the spectral lines. The spectrometer is assembled using a black cardboard frame. A narrow window with a width of approximately 2 mm is opened at the distal end of a cardboard tube, and a collimating slit is formed by placing two pieces of black electrical tape over the window. The transmission gratings, on the opposite side of the tube, disperse the beam of light entering through the slit into spectral lines with different colours at different angles.

The tube, in combination with the slit, acts to ensure that only approximately collimated light is focused onto the detector by the camera lens. For the calibration measurements, the spectrometer is pointed at a fluorescent commercial lamp.

The images of the spectra are acquired by a camera, then analysed with Tracker video analysis software.

The spectrum shows many peaks distributed over the range of wavelengths of visible light. We accurately measure the positions of their peaks using Tracker. For the reference value of the wavelength corresponding to each peak we use the results of measurements

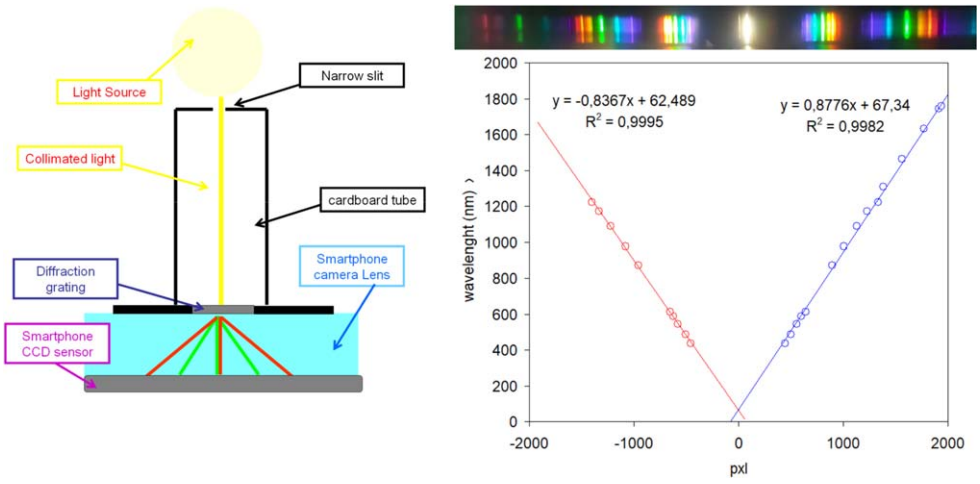

Figure A1. The spectrometer setup: a parallelepiped cardboard box with a hole for the lens of the camera on one side and a narrow window made affecting the cardboard with a cutter on the other side. Two pieces of black electrical tape are placed over the window to form a collimating slit. The light source is placed in front and properly centered with respect to the collimating slit. (B) The wavelength–pixel calibration curves of the $300\,\mathrm{l\,mm^{-1}}$ grating, based on the fluorescent lamp spectrum.

carried out with a high-resolution commercial spectrometer [29]. In figure A1 the positions of the peaks are plotted against their reference wavelengths and the points are shown to be adequately fit by a straight line and wavelength–pixel calibration curves show a coefficient of determination, R^2 of nearly 1. The uncertainty in the wavelength measurement inferred using this fit is a few nanometers.

ORCID iDs

P Onorato https://orcid.org/0000-0002-2110-7582

References

[1] Savall-Alemany F, Domènech-Blanco J L, Guisasola J and Martínez-Torregrosa J 2016 Identifying student and teacher difficulties in interpreting atomic spectra using a quantum model of emission and absorption of radiation *Phys. Rev. Phys. Educ. Res.* **12** 010132
[2] Colantonio A, Galano S, Leccia S, Puddu E and Testa I 2017 A teaching module about stellar structure and evolution *Phys. Educ.* **52** 015012
[3] Colantonio A, Galano S, Leccia S, Puddu E and Testa I 2018 Design and development of a learning progression about stellar structure and evolution *Phys. Rev. Phys. Educ. Res.* **14** 010143
[4] Bonanno A, Bozzo G, Stranges F and Sapia P 2018 Physics meets fine arts: a project-based learning path on infrared imaging *Eur. J. Phys.* **39** 025805
Bonanno A, Bozzo G, Stranges F and Sapia P 2017 *La Riflettografia Infrarossa tra Fisica, Arte e Tecnologia G. Fis.* **LVIII** 27 (in Italian)
[5] Daffara C, De Manincor N, Perlini L, Bozzo G, Sapia P and Monti F 2019 Infrared vision of artworks based on web cameras: a cross-disciplinary laboratory of optics *J. Phys. Conf. Ser.* **1287** 012018
[6] Lorenz R D 2014 A simple webcam spectrograph *Am. J. Phys.* **82** 169–73
[7] Onorato P, Malgieri M and De Ambrosis A 2015 Measuring the hydrogen Balmer series and Rydberg's constant with a home made spectrophotometer *Eur. J. Phys.* **36** 058001
[8] Rosi T, Malgieri M, Onorato P E and Oss S 2016 What are we looking at when we say magenta ? Quantitative measurements of RGB and CMYK colours with a homemade spectrophotometer *Eur. J. Phys.* **37** 065301
[9] Scheeline A 2010 Teaching, learning, and using spectroscopy with commercial, off-the-shelf technology *Appl. Spectrosc.* **64** 256A–58AA
[10] Rodrigues M, Marques M B and Carvalho P S 2014 Teaching optical phenomena with Tracker *Education* **49** 671–7
Rodrigues M, Marques M B and Carvalho P S 2015 Measuring and teaching light spectrum using Tracker as a spectrographs *Education and Training in Optics and Photonics (ETOP)* **2015** 97931L -97931L-6
Rodrigues M, Marques M B and Carvalho P S 2015 How to build a low cost spectrographs with Tracker for teaching light spectra *Physics Education* **51** 014002
[11] Grove T T, Millspaw J, Tomek E, Manns R and Masters M 2018 Using a shoebox spectrograph to investigate the differences between reflection and emission *American Journal of Physics* **86** 594
[12] Onorato P, Malgieri M. and e De Ambrosis A Quantitative analysis of transmittance and photoluminescence using a low cost apparatus *Eur. J. Phys.* **37** 2015015301
[13] Smith Z J, Chu K, Espenson A R, Rahimzadeh M, Gryshuk A, Molinaro M, Dwyre D M, Lane S, Matthews D and Wachsmann-Hogiu S 2011 Cell-phone-based platform for biomedical device development and education applications *PLoS One* **6** e1570
[14] Kiisk V 2014 An educational spectrograph using a digital camera as a training aid for physics students *Eur. J. Phys.* **35** 035013
[15] Brown D and Cox A J 2009 Innovative uses of video analysis *Phys. Teach.* **47** 145–50
[16] Cross P C, Wilson E B Jr and Decius J C 2002 Molecular vibrations: the theory of infrared and raman vibrational spectra *The Raman Effect: A Unified Treatment of the Theory of Raman Scattering by Molecules* ed Derek A Long (New York: Wiley) (2001)

[17] Thornton S T and Rex A 1993 *Modern Physics for Scientists and Engineers* (Philadelphia, PA: Saunders College Publishing)
[18] Bernath P F 2005 Light scattering and the Raman effect *Spectra of Atoms and Molecules* ed P F Bernath 2nd edn (New York: Oxford University Press Inc.) pp 293–317
Ferraro J R, Nakamoto K and Brown C W (ed) 2003 *Introductory Raman Spectroscopy* 2nd edn (San Diego, CA: Academic)
Abramczyk H 2005 *Introduction to Laser Spectroscopy* (New York: Elsevier Science Ltd)
[19] Schott AG 2020 Optical filter glass (https://schott.com/advanced_optics/english/products/optical-components/optical-filters/optical-filter-glass/index.html)
[20] Faris G W and Copeland R A 1997 Wavelength dependence of the Raman cross section for liquid water *Appl. Opt.* **36** 2686–8
[21] NIH 2019 ImageJ: Image processing and analysis in Java (https://imagej.nih.gov/ij/)
[22] Rossi M, Gratton L M and Oss S 2013 Bringing the digital camera to the physics lab *Phys. Teach.* **51** 141–3
[23] ITU-R 2002 *Recommendation BT.709-5: Parameter Values for the HDTV Standards for Production and International Programme Exchange* (Geneva: International Telecommunication Union)
[24] Elliott K H and Mayhew C A 1998 The use of commercial CCD cameras as linear detectors in the physics undergraduate teaching laboratory *Eur. J. Phys.* **19** 107–17
[25] Palmer C 2014 *Diffraction Grating Handbook* 7th edn (New York: Newport Corp)
Harvey J E and Pfisterer R N 2019 Understanding diffraction grating behavior: including conical diffraction and Rayleigh anomalies from transmission gratings *Opt. Eng.* **58** 087105
[26] Larouche P, Max J-J and Chapados C 2008 Isotope effects in liquid water by infrared spectroscopy. II. Factor analysis of the temperature effect on H_2O and D_2O *J. Chem. Phys.* **129** 064503
[27] Choe C S, Lademann J and Darvin M E 2016 Depth profiles of hydrogen bound water molecule types and their relation to lipid and protein interaction in the human stratum corneum in vivo *Analyst* **141** 6329–37
[28] Kazuo N 1997 *Infrared and Raman Spectra of Inorganic and Coordination Compounds* 5th edn (New York: Wiley)
[29] Wikipedia 2020 Fluorescent lamp (https://en.wikipedia.org/wiki/Fluorescent_lamp#/media/File:Fluorescent_lighting_spectrum_peaks_labeled_with_colored_peaks_added.png)